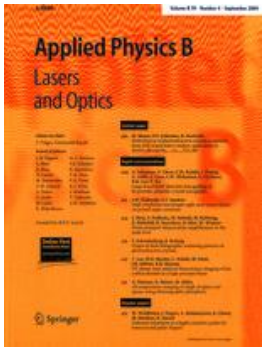

This article was published in:
M. A. Porras, Z. L. Horvath, and B. Major "On the use of lenses to focus fewcycle pulses with controlled carrier–envelope phas" *Applied Physics B: Lasers and Optics* 108(3) 521–531 (2012).
The final publication is available at Springer via http://dx.doi.org/10.1007/s00340-012-5073-y.

Applied Physics B: Lasers and Optics manuscript No.
(will be inserted by the editor)

On the use of lenses to focus few-cycle pulses with controlled carrier-envelope phase

Miguel A. Porras[1], Zoltan L. Horvath[2], Balazs Major[2]

[1] Departamento de Física Aplicada a los Recursos Naturales, Universidad Politécnica de Madrid, Rios Rosas 21, ES-28003, Spain.
e-mail: miguelangel.porras@upm.es, Fax: 34 91 3366952
[2] Department of Optics and Quantum Electronics, University of Szeged, P. O. Box 406, H-6701 Szeged, Hungary.

Received: / Revised version:

Abstract From a model of focusing with lenses that includes the effects of the lens variable thickness, material dispersion, aperture, spherical and chromatic aberrations, we characterize the conditions under which a lens can focus to few-cycle, transform-limited pulses propagating without distortion along the focal region. A lens also allows to control the carrier-envelope phase shift along the focus. The carrier-envelope phase shift is drastically reduced by focusing with specific focal lengths and input spot sizes, which are of the same order as those typically used in experiments involving focusing for phase-sensitive, light-matter interactions.

1 Introduction

In experiments involving focusing of visible or near-infrared pulses of duration of a few femtoseconds, comprising only a few oscillations of the electric field, the use of lenses is prevented because of the widespread belief that they strongly deteriorate the pulse quality. Elimination of the dispersion introduced by the variable lens thickness is thought to require sophisticated means, and the lens chromatic aberration is assumed to cause pulse broadening and pulse front distortion in the focus. To avoid having to deal with these undesirable effects, and to keep the bandwidth-limited duration of the input pulse in the focal region, reflective optics is usually used in experiments of high-harmonic generation with few-cycle driving pulses [1,2], in attosecond pulse generation [3,4], in other phase-sensitive interactions with matter [5–8], in devices that measure the carrier-envelope phase (CEP) of the pulse based on these phase-sensitive interactions [9–11], or in compression of femtosecond pulses by filamentation [12,13].

In the phase sensitive interactions with matter, it would be desirable to maintain, in principle, a constant CEP in the interaction region, or at least to know its variation along the focus to restrict the interaction region properly [14]. As it is well-known, the CEP experiences a total phase shift of $-\pi$ through the focal region due to Gouy phase shift, but the specific variation within focus depends on the focusing geometry. Focusing with a mirror (i.e., with no chromatic aberration), the CEP variation can be controlled only by imprinting suitable variations with frequency of the pulse spot size in front of the mirror [7,15], but this method is difficult to implement in practice. More recently, it has been shown that insertion of a dielectric slab in the focusing path may result in nearly constant CEP in the second half of the focal region [16], but as discussed below, this method only works for focal depths in the micrometer range. There are no previous studies on how the CEP varies along the focus of a lens.

The early studies on femtosecond pulse focusing with lenses dealt, in fact, with the spatial and temporal distortions of the focused pulse due to lens material dispersion, spherical and chromatic aberrations, to highlight the differences between quasi-monochromatic and short pulse focusing [17–22]. In addition, these studies consider uniform illumination [17–22], or Gaussian illumination with spot size comparable to the lens aperture [22], because an important concern was spatial resolution for applications such as scanning microscopy. The choice of ultraviolet carrier wave lengths to illustrate many examples [17,18] enhanced further the effects of chromatic aberration. Resolution is not a relevant concern in the above phase-sensitive interactions with matter. Mirrors are not uniformly illuminated, focusing is not too tight in HHG or attosecond pulse generation experiments, and wave lengths are typically in the near-infrared. To get an idea of the difference, the propagation time difference between the marginal and axial rays in a lens is a rough measure of pulse broadening at focus [17,18]. For a fused silica lens of radius $a = 1$ cm and focal length 10 cm that is uniformly illuminated with radiation at 800 nm, the propagation time difference is about 50 fs, much larger the duration ΔT of few-cycle pulses. When illuminated with spot size $s = 1$ mm, the propagation time difference between the "marginal" ray at s and the axial ray is instead 0.5 fs $\ll \Delta T$. In this case pulse broadening is expected to be inappreciable.

In this paper, we model focusing with lenses of few-cycle pulses with Gaussian transversal profile by means of a model based on a combination of geometrical and wave optics, similar to that introduced in Ref. [23], and that includes the effects of the lens aperture, its radially varying thickness, spherical and chromatic aberrations (Sec. 2). From this starting point, we first demonstrate that if the illuminated lens area is small enough, so that truncation by the lens aperture and the effects of spherical aberration are small, then the dispersion introduced by the lens material is substantially the same as that introduced by a dielectric slab with thickness equal to the lens center thickness (Sec. 3.1). Lens material dispersion then can be pre-compensated with standard pulse shaping techniques, even for the broad

bandwidths of pulses close to the single-cycle limit, if particularly thin lenses are used. Next we characterize the limit to the lens chromatic aberration below which the bandwidth-limited pulse obtained after the lens remains as such and propagates without distortion along the focal region (Sec. 3.2). Within this limit, we derive an approximate expression for the CEP shift along the focus of the lens (Sec. 4). We find that the chromatic aberration influences the CEP variation in the focus, and that a suitable (small) amount of chromatic aberration, introduced with specific focal lengths and input spot sizes, results in a constant CEP along the first half of the focus, and therefore in an invariable electric field in this region.

Through a series of examples, we show that the conditions for compensable lens material dispersion, for undistorted propagation of the bandwidth-limited pulse along the focus, and for frozen CEP in the first half of the focus, can be satisfied using standard lens materials, with focal lengths and input spot sizes of the same order as those used in experiments involving focusing for phase-sensitive interactions with matter, and along the typical millimetric focal depths used in these experiments.

Throughout this article, prime signs denote differentiation with respect to frequency, and subscripts 0 evaluation at the pulse carrier frequency ω_0. The symbols $\Delta\omega$ and ΔT denote FWHM of spectral and temporal intensity, respectively.

2 Accurate description of few-cycle pulse focusing with a lens

In our analysis of few-cycle pulse focusing with a lens, we follow the usual procedure of propagating the monochromatic constituents from the entrance plane of the lens up to the focal region, and superpose them to obtain the pulse shape in that region.

As illustrated in Fig. 1, the wave front emerging from the lens is that whose phase difference with the input plane wave front is $(\omega/c)nD$, where ω is the frequency of the selected monochromatic component, c the speed of light in vacuum, n the lens refraction index, and D its center thickness. The shape of the wave front is determined by tracing constant optical path nD rays starting from the input wave front at different distances from the optical axis. Snell's law is used at the two spherical surfaces of the lens so the effect of the lens thickness and its variation across the lens is accurately taken into account. The aberration function [24] is determined as the distance $\Gamma = \overline{Q'Q}$ between the point Q' on the emerging wave front and the point Q on the same ray on the reference sphere S, whose radius is equal to the back paraxial focal length f, defined as the distance from the lens back vertex to the paraxial focal point, and given by [24,25]

$$f = \left[(n-1)\left(\frac{1}{R_1}+\frac{1}{R_2}\right) - \frac{(n-1)^2}{n}\frac{D}{R_1R_2}\right]^{-1} - \frac{R_2D}{n(R_1+R_2-D)+D}\,, \tag{1}$$

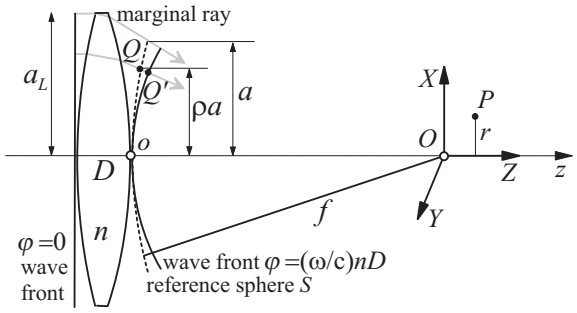

Fig. 1 Geometrical construction, parameters and coordinate systems for the evaluation of the focused monochromatic disturbances from the input plane, monochromatic disturbance.

with the sign convention that the front and back surface radii, R_1 and R_2, are positive if they are convex, and negative if concave. The aperture a of the reference sphere is determined from the intersection of the input marginal ray at the lens radius a_L with the reference sphere. If the distance of a typical point on the reference sphere from the optical axis is denoted by ρa with ρ ranging from zero to unity, the primary spherical aberration coefficient B is obtained by fitting the aberration function $\Gamma(\rho)$ with the fourth-order polynomial $B\rho^4$. Note that the spherical aberration coefficient B, the aperture a, and f depend on frequency because of the dependence of n with frequency. In practice, all values of a are close to a_L.

The monochromatic disturbance at the reference sphere can then be written as $E_S(\omega,\rho) = p(\omega)e^{-(a\rho/s)^2}e^{i(\omega/c)[nD+B\rho^4]}$, where $p(\omega)$ carries the amplitude and phase of each monochromatic component at the input wave front. For the few-cycle pulses in this paper, $p(\omega)$ is a broad function of large bandwidth $\Delta\omega$ about the optical or near infrared carrier frequency ω_0. The transversal amplitude distribution is assumed to be the Gaussian function $e^{-(a\rho/s)^2} = e^{-\kappa\rho^2}$, where the spot size s depends in general on frequency, and we have introduced the truncation parameter $\kappa = (a/s)^2$ in the second expression.

Once the disturbance at the reference sphere is found, the disturbance at a point P in the vicinity of the focus, placed at an axial distance z from the lens back vertex and at a distance r from the lens axis, is given by the Huygens-Fresnel integral

$$E(\omega,r,z) = \frac{-i}{\lambda}\iint_S E_S(\omega,\rho)\frac{e^{i(\omega/c)d}}{d}dS\,, \tag{2}$$

where $\lambda = 2\pi c/\omega$ is the vacuum wave length, the integral extends to the reference sphere S, and $d = \overline{QP}$. In our case,

$$E(\omega,r,z) = \frac{-i}{\lambda}p(\omega)e^{i\frac{\omega}{c}nD}\iint_S e^{-\kappa\rho^2}\frac{e^{i\frac{\omega}{c}[d+B\rho^4]}}{d}dS\,. \tag{3}$$

This integral is the same as that in Ref. [24] for the study of the three-dimensional light distribution near focus except for the Gaussian and aberration factors. Thus, following the same procedure as in Ref. [24], and particularizing to $r = 0$, we obtain the on-axis disturbance for the frequency ω as

$$E(\omega, z) = \frac{-i\omega a^2}{2cf} p(\omega) e^{i\frac{\omega}{c}(nD+z)} I(u)\,, \tag{4}$$

where

$$I(u) = 2\int_0^1 e^{-\kappa\rho^2} e^{i\left[\frac{\omega}{c}B\rho^4 - \frac{u}{2}\rho^2\right]} \rho d\rho\,, \tag{5}$$

and $u = (\omega/c)(a/f)^2(z-f)$ is the axial optical coordinate. Equations (4) and (5) involve the Fresnel approximation, which is very accurate in all cases of interest, and the Debye approximation. In all cases we will consider, the input spot size s is sizably smaller than $a \simeq a_L$, in which case the Debye approximation is accurate if $s^2/\lambda f \gg 1$ [24], implying that the focal shift from the geometrical focus $z = f$ is negligible. This condition is well satisfied for the input spot sizes and focal lengths considered below.

The integral $I(u)$ can be evaluated either numerically or analytically in terms of Fresnel sine and cosine integrals [24] of complex arguments (due to the Gaussian factor), which in turn can be expressed in terms of the error functions with complex arguments [26]. For $B \neq 0$, the analytical result is

$$I(u) = e^{-i\frac{\hat{u}^2}{16\beta}} \left(\frac{\pi}{2|\beta|}\right)^{\frac{1}{2}} \frac{1 + i\,\mathrm{sgn}(\beta)}{2} \times \tag{6}$$
$$\times \left\{ \mathrm{erf}\left[\frac{1 - i\,\mathrm{sgn}(\beta)}{2}(2|\beta|)^{\frac{1}{2}}\left(1 - \frac{\hat{u}}{4\beta}\right)\right] + \mathrm{erf}\left[\frac{1 - i\,\mathrm{sgn}(\beta)}{2}(2|\beta|)^{\frac{1}{2}}\frac{\hat{u}}{4\beta}\right]\right\},$$

where $\hat{u} = u - 2i\kappa$, and $\beta = (\omega/c)B$.

In short, Eqs. (4) and (6), with the focal length in Eq. (1), with the refractive index given by a Sellmeier relation [27], and the spherical aberration coefficient B and aperture a determined by ray tracing from Snell's law, provide an accurate description of the focused monochromatic constituents that includes the effects of the lens thickness and its variation with radial distance, the effects of the lens aperture and of its spherical and chromatic aberrations. Given the spot size s and complex weight p of each input Gaussian monochromatic components, the inverse Fourier transform of $E(\omega, z)$ yields the on-axis pulse form taking into account all these effects. This detailed description of few-cycle pulse focusing with a lens is the starting point of our analysis, and will be repeatedly used below for the accurate computation of the pulse temporal form along the focal region in order to check the validity of our results.

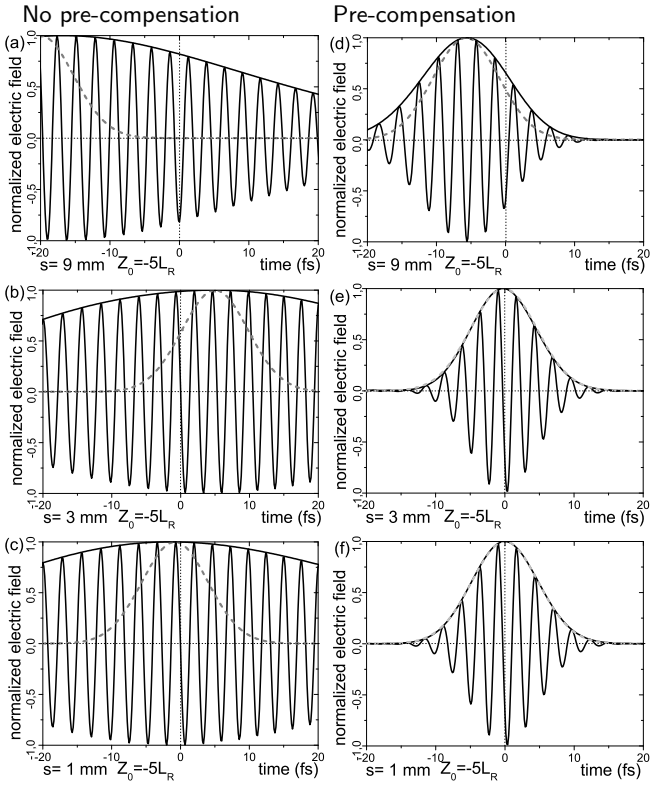

Fig. 2 Pulse shapes and envelopes after the lens and before the focal region (see text for lens and input pulse details) without and with pre-compensation of the lens center thickness GDD and TOD for different input spot sizes. Solid black curves: The particular axial points where the pulse shapes are shown are $Z_0 = z - f_0 = -5L_{R,0}$ with $L_{R,0} = 2cf_0^2/\omega_0 s_0^2$. Dashed gray curves: transform-limited Gaussian pulse of duration $\Delta T = 8$ fs. All pulses are normalized to unit amplitude. Time is zero at the instant of arrival of a plane pulse of the same carrier frequency at the a position z. The transform-limited Gaussian pulse is conveniently shifted in time in each figure for a better comparison.

3 Focusing to transform-limited, non-reshaping, few-cycle pulses with a lens

3.1 Compensation for the lens material dispersion

Assume that the lens aperture a_L is sufficiently large compared with the Gaussian spot size s so that the effects of the lens aperture and spherical aberration can be neglected. The factor $e^{i(\omega/c)B\rho^4}$ accounting for spherical aberration in integral $I(u)$ in Eq. (5) can be neglected if $|B\rho^4| < 0.9\lambda$ [24]. For uniform illumination, this condition requires $B < 0.9\lambda$, since $\rho \leq 1$. For Gaussian illumination, however, the maximum value of ρ with significant in-

tensity is about s/a_L, and the condition of negligible spherical aberration becomes $|B(s/a_L)^4| < 0.9\lambda$, which can always be satisfied for sufficiently large lens radius a_L or small spot size s. Neglecting then the factor $e^{i(\omega/c)B\rho^4}$, integral $I(u)$ in Eq. (5) reduces to $I(u) = (e^{-\kappa - iu/2} - 1)/(-\kappa - iu/2)$, which behaves as $I(u) \simeq 1/(\kappa + iu/2)$ for large truncation parameter κ ($a \gg s$). Introducing the Rayleigh range of the focused Gaussian beam and the axial coordinate with origin at the geometrical focus at the given frequency,

$$L_R = \frac{2cf^2}{\omega s^2}\,, \quad Z = z - f\,, \tag{7}$$

respectively, we can also write $I(u) \simeq (s/a)^2[L_R/(L_R + iZ)]$, and from Eq. (4),

$$E(\omega, z) \simeq p(\omega) e^{i\frac{\omega}{c}nD} e^{i\frac{\omega}{c}z} \frac{-f}{Z - iL_R}\,. \tag{8}$$

This is the usual formula that would be obtained from the standard Gaussian beam formalism [28], in which the effect of the lens thickness is reduced to introduce the phase $(\omega/c)nD$ corresponding to an optical length equal to the lens center thickness D, and the effect of the lens chromatic aberration is taken into account by the variation of the focal length with frequency. We can then conclude that that if the effects of spherical aberration and aperture are negligible, then a real lens acts as a slab of thickness equal to the lens center thickness D and an ideal lens of focal length f and vanishing thickness.

From a practical point of view, this means that to eliminate unwanted dispersive effects caused by the propagation of the pulse through the lens material it is enough to eliminate only those due to propagation a distance equal to the lens center thickness. For the typical spot sizes of the order of one millimeters used in experiments, lens apertures must be of the order of centimeters for aperture and spherical aberration effects to be negligible. Thicknesses of lenses with these apertures and typical focal lengths of tens of centimeters are of the order of millimeters. For the broad band spectra $p(\omega)$ of pulses with a few carrier oscillations, group-delay dispersion (GDD) and third-order dispersion (TOD) opposite to those introduced by a few millimeters of typical glasses can be easily introduced by using standard pulse shaping techniques, as chirped mirrors, and generally suffice to obtain a nearly transform-limited pulse after the lens. Approaching the single-cycle limit, particularly thin lenses could be needed for pre-compensation to be possible, as seen in the example in Sec. 4.

Figure 2 illustrates the above considerations in the case of a real lens made of fused silica, taken from the commercial catalog in Ref. [29] (center thickness $D = 3.78$ mm, aperture $a_L = 12.5$ mm, surface radii $R_1 = R_2 = 91.08$), and with paraxial back focal length $f_0 = 98.9$ mm at the pulse carrier frequency $\omega_0 = 2.355$ fs^{-1} ($\lambda_0 = 800$ nm). All pulse shapes after the lens shown in the figures (solid black curves) are calculated following the procedure described in Sec. 2. The input spot sizes $s = s_0 = 9, 3$ and 1 mm (independent of frequency) decrease from the top to the bottom panels.

Figures 2(a), (b) and (c) on the left side show the pulse shapes at a point after the lens, but before the focal region, in the case that a transform-limited, three-cycle, Gaussian pulse of duration $\Delta T = 8$ fs and spectrum $p(\omega) = \exp[-\Delta T^2(\omega-\omega_0)^2/8\ln 2]$ is launched on the lens. For reference, this transform-limited Gaussian pulse is plotted in all figures (dashed gray curves). For all three input spot sizes, the pulse after the lens is enormously broadened by the lens dispersion. Figures 2(d), (e) and (f) on the right show the pulse shapes at the same points after the lens in case that pre-compensation for the dispersion (GDD and TOD) of the lens center thickness is introduced in the input pulse, i. e., the spectrum of the input pulse is $p(\omega) = \exp[-\Delta T^2(\omega-\omega_0)^2/8\ln 2]\exp[-i\varphi_0''(\omega-\omega_0)^2/2 - i\varphi_0'''(\omega-\omega_0)^3/6]$, with $\varphi_0'' = 137$ fs^2 and $\varphi_0''' = 110$ fs^3. For the largest input spot size $s = 9$ mm, spherical aberration is significant ($|B_0(s_0/a_L)^4| \simeq 3.6\lambda_0 > 0.9\lambda_0$ at ω_0, and similar values for other frequencies). The pulse after the lens is significantly shortened, but pre-compensation for the dispersion of the lens center thickness is not sufficient to eliminate the actual dispersive effects of the lens due to its variable thickness [Fig. 2(d)]. On the contrary, for spot sizes $s = 3$ mm and $s = 1$ mm, spherical aberration is negligible ($|B_0(s_0/a_L)^4| \simeq 0.04\lambda_0$ and $|B_0(s_0/a_L)^4| \simeq 5\times10^{-4}\lambda_0$, respectively), and pre-compensation for the lens center thickness dispersion suffices to produce an approximately transform-limited Gaussian pulse of duration $\Delta T = 8$ fs after the lens [Figs. 2(e) and (f)].

3.2 Minimizing pulse reshaping in the focal region

Even if a nearly transform-limited, few-cycle pulse is obtained after the lens by pre-compensation, its chromatic aberration can result in severe pulse broadening and reshaping during propagation through the focal region [17–22]. In a converging lens, bluer spectral components are focused at shorter distances than redder components. This causes a z-dependent spectral filtering of the spectrum, that becomes shifted from ω_0 and narrowed, and that is observed as z-dependent blue or red shift of the carrier oscillations and pulse broadening.

Though the lens chromatic aberration can not be completely eliminated, its effect reshaping can be minimized, and could be beneficial for the control of the CEP, as discussed in Sec. 4. Envelope reshaping through the focal region is expected to be small for focusing conditions such that the variation with frequency of the focal length across the bandwidth $\Delta\omega$ is much smaller than the focal depth $2L_{R,0}$, that is, $|\Delta f| \simeq |f_0'|\Delta\omega \ll 2L_{R,0}$. Introducing the dimensionless parameter

$$\gamma \equiv \frac{f_0'}{L_{R,0}}\omega_0\,, \tag{9}$$

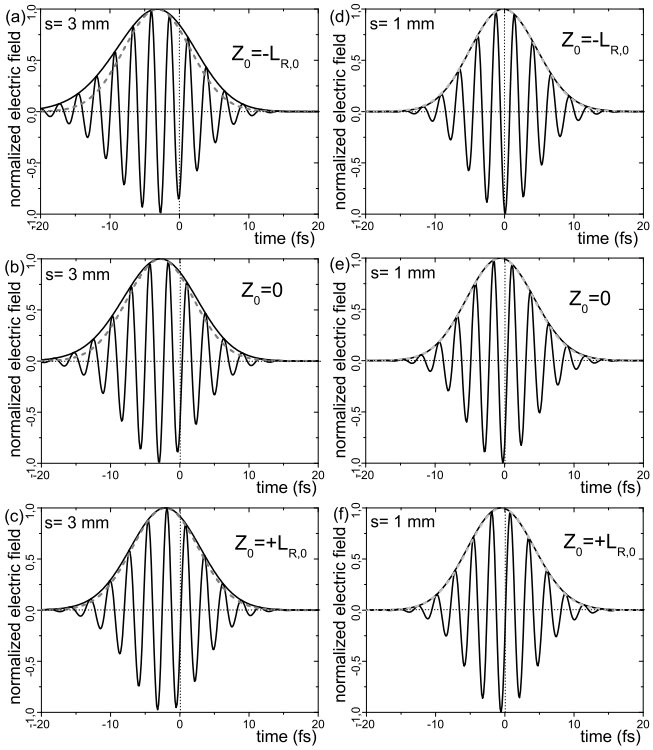

Fig. 3 Pulse shapes and envelopes at $Z_0 = -L_{R,0}, 0$ and $Z_0 = +L_{R,0}$ in the focal region (see text for lens and input pulse details) for the two input spot sizes $s_0 = 3$ mm and $s_0 = 1$ mm in Fig. 2 for which pre-compensation for the lens center thickness GDD and TOD produces a transform-limited pulse after the lens. The dashed gray curves represent transform-limited Gaussian pulse of duration $\Delta T = 8$ fs. All pulses are normalized to unit amplitude. Time is zero at the instant of arrival of a plane pulse of the same carrier frequency at each position z. The transform-limited Gaussian pulse is conveniently shifted in time in each figure for a better comparison.

and the relation $\Delta\omega = 2.773/\Delta T$ between the bandwidth and duration of a transform-limited pulse, the above condition reads

$$|\gamma| \ll \frac{\omega_0 \Delta T}{2.773}\,. \tag{10}$$

Noticeably, this condition can also be obtained by imposing that the propagation time difference from the input plane of the lens to the focus $|(s_0^2/2cf_0^2)\omega_0 f_0'| = |f_0'/L_{R,0}|$ between an ray at s_0 and an axial ray due to the lens chromatic aberration is much smaller than the pulse duration ΔT [17–19], as discussed in the introduction.

Fig. 3 continues the example of Fig. 2, and shows pulse shapes in the focal region in the two cases ($s = 3$ mm and $s = 1$ mm) in which transform-limited

pulses were obtained after the lens by pre-compensation. The derivative of the focal length at the carrier frequency can be approached by $f_0' \simeq -[n_0'/(n_0-1)]f_0 = -1.29$ mm fs from the thin lens approximation to the focal length in Eq. (1). For input spot size $s = 3$ mm, $L_{R,0} = 0.282$ mm, yielding $|\gamma| \simeq |-10.8| > \omega_0 \Delta T/2.773 \simeq 6.8$. Accordingly, the pulse is seen in Figs. 3(a), (b) and (c) to broaden and to reshape along the focal region due to the lens chromatic aberration. Instead, for input spot size $s = 1$ mm, $L_{R,0} = 2.54$ mm, and $|\gamma| \simeq |-1.2| \ll \omega_0 \Delta T/2.773 = 6.8$. As seen in Figs. 3(d), (e) and (f), broadening and reshaping along the focal region is not appreciable at the scale of the figure. The pulse continues to be a nearly transform-limited of duration $\Delta T \simeq 8$ fs in the entire focal region, the only appreciable changes being envelope and carrier temporal shifts due to the different group and phase velocities of the pulse, and therefore CEP shifts.

4 THE CEP SHIFT OF FEW-CYCLE PULSES ABOUT THE FOCUS OF A LENS

In this section we obtain an approximate analytical expression for the CEP shift along the focal region of the lens under the above conditions of negligible broadening and reshaping in the focal region of the lens. Following the perturbation theory developed in [30] for the effects of diffraction or focusing in the shape of few-cycle pulses, the monochromatic disturbance in Eq. (8) is written as

$$E(\omega, z) = p(\omega) e^{i\frac{\omega}{c}nD} \alpha(\omega, z) e^{i\varphi(z)} , \tag{11}$$

where the space-dependent amplitude $\alpha(\omega, z)$ and phase $\varphi(\omega, z)$ of the monochromatic Gaussian beam are given by

$$\alpha(\omega, z) = \frac{f}{L_R} \frac{1}{\sqrt{1 + (Z/L_R)^2}} , \tag{12}$$

$$\varphi(\omega, z) = \frac{\omega}{c} z - \frac{\pi}{2} - \tan^{-1}\left(\frac{Z}{L_R}\right) , \tag{13}$$

and where the last term is Gouy phase shift about the focus. The spectral phase is approached with $\varphi(\omega, z) = \varphi(\omega_0, z) + \varphi'(\omega_0, z)(\omega - \omega_0) + \varphi''(\omega_0, z)(\omega - \omega_0)^2/2$ in order to express the pulse temporal shape in the form of the enveloped carrier oscillations

$$E(t, z) = A(\tau, z) e^{-i[\omega_0 t - \varphi(\omega_0, z)]} , \tag{14}$$

where $\tau = t - \varphi'(\omega_0, z)$ is the local time at position z, and where the envelope is given by

$$A(\tau, z) = \int d\omega p(\omega) e^{i\frac{\omega}{c}nD} \alpha(\omega, z) e^{\frac{i}{2}(\omega-\omega_0)^2 \varphi''(\omega_0, z)} e^{-i(\omega-\omega_0)\tau} . \tag{15}$$

Pulse broadening due to the focusing process is accounted for by the factor with $\varphi''(\omega_0, z)$ [30], and can be neglected under the focusing conditions described in the preceding section. The spectral amplitude is also approached by $\alpha(\omega, z) = \alpha(\omega_0, z) + \alpha'(\omega_0, z)(\omega - \omega_0)$ to obtain

$$A(\tau, z) = \alpha(\omega_0, z)A(\tau) + i\alpha'(\omega_0, z)\frac{dA(\tau)}{d\tau}\,, \tag{16}$$

where

$$A(\tau) = \int d\omega p(\omega) e^{i\frac{\omega}{c}nD} e^{-i(\omega-\omega_0)\tau} \tag{17}$$

is the envelope just after the lens. The second term in Eq. (16) describes envelope reshaping along the focal region due to the focusing process [30] and, in particular, due to the spectral filtering caused by the chromatic aberration. Under the conditions explained in the preceding section, the envelope in Eq. (16) can be approached by $A(\tau, z) \simeq \alpha(\omega_0, z)A(\tau) = \alpha(\omega_0, z)A[t - \varphi'(\omega_0, z)]$, that is, by an invariable temporal shape with a z-dependent amplitude and a z-dependent temporal shift.

The CEP at a point z is the phase of the carrier oscillations at the time at which the amplitude $|A(\tau, z)|$ is maximum (assuming there is only one). Then, if this time is τ_p at a position z in the focal region, the CEP at z is given, from Eq. (14), by $\Phi(z) = -\omega_0[\tau_p + \varphi'(\omega_0, z)] + \varphi(\omega_0, z) + \phi$, where ϕ is the phase of $A(\tau_p, z)$. Under the condition of negligible envelope reshaping during propagation through the focus, the peak local time τ_p and phase ϕ are the same at any z. The CEP shift $\Delta\Phi(z)$, taking the geometrical focus at the carrier frequency f_0 as a convenient reference point, is then simply given by

$$\begin{aligned}\Delta\Phi(z) = &[-\omega_0\varphi'(\omega_0, z) + \varphi(\omega_0, z)] \\ &- [-\omega_0\varphi'(\omega_0, f_0) + \varphi(\omega_0, f_0)]\,.\end{aligned} \tag{18}$$

The CEP shift in this equation reflects the difference between the phase and group velocities of the pulse, which originates from, but is not equal to, Gouy phase shift of the monochromatic components along the focus, the specific CEP variation depending on the input pulse, on how it is focused [7,15,16], and in our case, on the lens chromatic aberration.

Evaluation of the CEP shift from Eq. (18) is a straightforward calculation of derivatives of the spectral phase in Eq. (13), which becomes, however, quite involved if L_R, f and $Z = z - f$ are functions of frequency because of the lens chromatic aberration. The result of these long calculations is

$$\Delta\Phi(z) = -\tan^{-1}\left(\frac{Z_0}{L_{R,0}}\right) + \frac{1}{1 + \left(\frac{Z_0}{L_{R,0}}\right)^2}\left[g\left(\frac{Z_0}{L_{R,0}}\right) + \gamma\left(\frac{Z_0}{L_{R,0}}\right)^2\right], \tag{19}$$

where $Z_0 = z - f_0$ is the axial distance from the geometrical focus at the carrier frequency,

$$g = -\frac{L'_{R,0}}{L_{R,0}}\omega_0 \simeq 1 + 2\frac{s'_0}{s_0}\omega_0 + 2\frac{n'_0}{n_0 - 1}\omega_0 \simeq 1 + 2\frac{s'_0}{s_0}\omega_0\,, \tag{20}$$

and γ is given by Eq. (9), or by

$$\gamma \simeq -\frac{n_0'}{n_0-1}\frac{f_0}{L_{R,0}}\omega_0\,. \tag{21}$$

For the approximate equalities in Eqs. (20) and (21) we have used the relation $f_0' = -[n_0'/(n_0-1)]f_0$ obtained from the thin lens approximation to Eq. (1). An expression similar to Eq. (19) has been previously obtained for focusing without chromatic aberration [15], e. g., with a spherical mirror, and also for focusing with a mirror inserting a dielectric dispersive slab in the focusing path for the purpose of controlling the CEP shift through the focus [16]. Eq. (19) is expected to hold under the condition of negligible envelope reshaping along the focal region, and therefore requires small chromatic aberration such that $|\gamma| \ll \omega_0 \Delta T/2.773$, as explained in the preceding section.

The approximate linear variation of the CEP with negative slope -1 (in units of $L_{R,0}$) due to Gouy phase shift $-\tan^{-1}(Z_0/L_{R,0})$ is modified by the approximate linear variation with of the term with g. Both linear variations compensate when $g = 1$. The contribution to the value of g of the term with $2n_0'\omega_0/(n_0-1)$ in Eq. (20) is negligible for any real lens, so that in practice $g \simeq 1+2(s_0'/s_0)\omega_0$ depends only on the possible variation with frequency of the spot size of the Gaussian beam components in front of the lens [15]. For example $g = 1$ corresponds to the simplest hypothesis of an input pulsed Gaussian beam with constant spot size (s = const.). However, $g = 0$, i.e., an input isodiffracting pulsed Gaussian beam (constant Rayleigh range) [31,32] fits better experimental observations, in which values of the CEP shift compatible with Gouy phase shift were measured [7,11]. We will then take $g = 0$ as the most realistic value and for simplicity in the illustrative examples below, though the considerations about the CEP control hold irrespective of the value of g with straightforward modifications.

The term with γ introduces an approximate quadratic variation of the CEP, and already appeared in the form $\gamma = (n_0'\delta/n_0^2 L_{R,0})\omega_0$ as the result of placing a dielectric slab of thickness δ and refractive index n between a spherical mirror and the focal region [16]. Values of γ of the order of unity were shown to result in a nearly constant CEP in the second half of the focal region. The required slab thickness for this effect to take place takes a reasonable value of the order of a millimeter in half focal depths $L_{R,0}$ of several tens of micrometers [16], but of the order of a meter for the half focal depths in the millimeter range used in most of experiments, what renders the slab method useless in these cases.

Here, the term with the quadratic variation originates from the chromatic aberration of the lens. For lens materials in their transparency region, $n_0' > 0$, so that $\gamma < 0$. In the example of Fig. 4, the CEP shift in absence of chromatic aberration, i. e., with $\gamma = 0$ is equal to Gouy phase shift, but the CEP with small chromatic aberration such that $\gamma = -1$ is nearly constant in the first half of the focus. Note that $|\gamma| = 1 \ll \Delta T\omega_0/2.773$ down to single-cycle pulses at typical carrier frequencies, and therefore this small

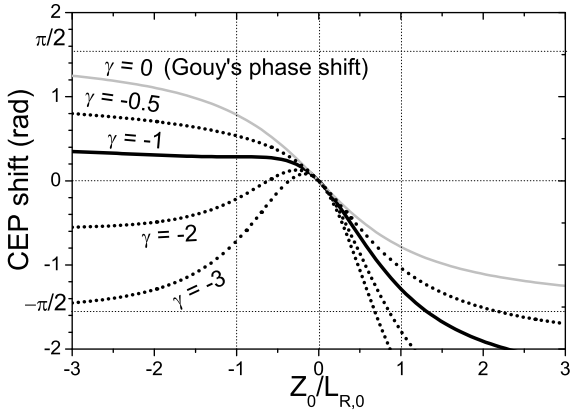

Fig. 4 Prediction of Eq. (19) for the CEP shift from the focus for input isodiffracting pulsed Gaussian beam ($g = 0$) and increasing (but small) chromatic aberration $\gamma = 0, -0.5, -1, -2$ and -3. The value $\gamma = -1$ produces a nearly constant CEP in the first half of the focal region.

chromatic aberration does not involve appreciable pulse broadening or reshaping along the focal region. The effect of nearly constant CEP in the first half of the focus can be understood from the fact that higher frequencies in the spectrum are focused at focal lengths $f < f_0$. In their particular focus, these frequencies are both enhanced in amplitude, and shifted towards the leading part of the pulse due to their Gouy phase shift. The result is an increase of the pulse group velocity, which can then match the pulse superluminal phase velocity about the focus, reducing the CEP variation.

In a practical application, one may wish to obtain this effect in a given half depth of focus $L_{R,0}$. The condition $\gamma = -1$ of nearly constant CEP, with γ given by Eq. (21), in a length $L_{R,0} = 2cf_0^2/\omega_0 s_0^2$, is satisfied with focal length and input spot size

$$f_0 = \frac{n_0 - 1}{n_0'} \frac{L_{R,0}}{\omega_0}, \quad s_0 = \sqrt{\frac{2cf_0^2}{\omega_0 L_{R,0}}}. \tag{22}$$

Note that the focal length and input spot size for constant CEP in given $L_{R,0}$ are completely determined by the dispersive properties of the lens material at the carrier frequency. According to Eq. (22), these focal length and input spot size are larger as the lens material has higher refraction index and as is less dispersive. For example, pulses at 800 nm will focus to constant CEP in $L_R = 3$ mm using a fused silica lens ($n_0 = 1.453$, $n_0'\omega_0 = 0.014$) of focal length $f_0 = 9.8$ cm illuminated with spot size $s_0 = 0.91$ mm, or using a potassium fluoride lens ($n_0 = 1.36$, $n_0'\omega_0 = 6.2 \times 10^{-3}$) with $f_0 = 17.3$ cm and $s_0 = 1.60$ mm. The values of n_0 and n_0' for the evaluation of f_0 and s_0 are taken from corresponding Sellmeier relations [27].

For CEP-sensitive interactions with matter involving extremely powerful laser pulses, as in HHG or attosecond pulse generation experiments, focal lengths of the order of a meter and input spot sizes in the centimeter range are desirable in order to minimize nonlinear and heating effects in the lens. Fused silica, potassium fluoride, or BK7 lenses with these large focal lengths and input spot sizes will induce larger chromatic aberration, and hence faster variation of the CEP, as in Fig. 4 for $\gamma < -1$. To freeze the CEP with input spot sizes of the order of a centimeter, one may instead use a Thallium Bromide/Chloride (KRS-6) lens with the high refraction index $n_0 = 2.196$ and low dispersion $n_0'\omega_0 = 1.61 \times 10^{-3}$ at 800 nm, yielding the large focal length $f_0 = 2.223$ m and input input spot size $s_0 = 2.05$ cm for $L_{R,0} = 3$ mm, or $f_0 = 1.111$ m and $s_0 = 1.45$ cm for $L_{R,0} = 1.5$ mm. In these cases, the lens aperture must be large enough to avoid truncation and spherical aberration effects. Other materials, or several materials in a doublet, can be investigated to control the chromatic aberration, fitting f_0 and s_0 to experimental requirements. A detailed study of these combinations is beyond the scope of this paper.

Figure 5 illustrates all preceding results with the example of focusing to a transform-limited, propagation-invariant pulse of duration $\Delta T = 4$ fs at 800 nm carrier wave length (one and a half cycle) with a nearly constant CEP in a length $L_{R,0} = 3$ mm by using a CaF_2 lens. From Eq. (22), the needed focal length and spot size for $\gamma = -1$ in $L_{R,0} = 3$ mm are $f_0 = 15.359$ cm and $s_0 = 1.422$ mm. A CaF_2 lens with this focal length can be constructed, for instance, with equal surface radii $R_1 = R_2 = 133.018$ cm and center thickness $D = 0.7$ mm. This small thickness is chosen in order that GDD and TOD are the only significant dispersive effects for the 4 fs long pulse, at the same time that the lens radius a_L can be even much larger than s_0. The maximum lens radius of a lens with these surface radii and thickness is 9.641 mm, so that we can set $a_L = 9.0$ mm $\gg s_0$. The spectrum of the input pulse is then $p(\omega) = \exp[-\Delta T^2(\omega-\omega_0)^2/8\ln 2]\exp[-i\varphi_0''(\omega-\omega_0)^2/2 - i\varphi_0'''(\omega-\omega_0)^3/6]$, where $\varphi_0'' = 20.2$ fs^2 and $\varphi_0''' = 14.0$ fs^3 compensate for the lens center thickness GDD and TOD, and the input spot size $s = s_0(\omega_0/\omega)^{0.5}$ presents the characteristic dependence on frequency of isodiffracting pulsed Gaussian beams ($g = 0$).

Figure 5(a) depicts the CEP evolution along the focal region, evaluated from the approximate formula in Eq. (19) (solid curve), and extracted directly from the pulse temporal shapes along the focal region (closed circles), which are calculated from the rigorous procedure of Sec. 2. For the input isodiffracting Gaussian pulsed beam, the CEP evolution in absence of chromatic aberration coincides with Gouy phase shift (dashed curve). The approximate formula in Eq. (19) reproduces accurately the actual CEP evolution, since the condition of negligible envelope reshaping $|\gamma| = 1 \ll \omega_0\Delta T = 3.4$ is satisfied. In particular, the CEP is seen in Fig. 5(a) to remain approximately constant in the first 3 mm of the focal region. Figs. 5 (b), (c) and (d) confirm that the envelope does not appreciably change from the entrance to the exit of the focal region (black solid curves)

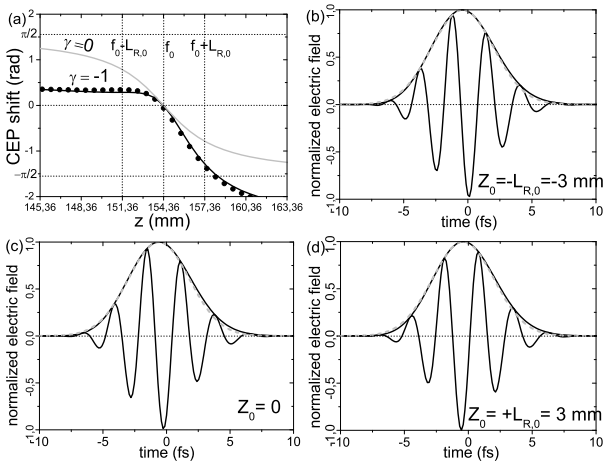

Fig. 5 For the input pulse and lens specified in the text, (a) CEP shift along the focal region predicted by Eq. (19) (black solid curve), exact CEP shift obtained from the temporal pulse forms along the focal region calculated numerically (closed circles), and CEP shift in absence of any chromatic aberration (gray solid curve); (b) (c) and (d) pulse shapes and envelopes at the entrance, middle and exit of the focal region (solid curves), and the envelope of a transform-limited Gaussian pulse of duration $\Delta T = 4$ fs (gray dashed curve). Time is zero at the instant of arrival of a plane pulse of the same carrier frequency at each position. The transform-limited Gaussian pulse is differently shifted in time in each figure for a better comparison.

and does not differ substantially from that of the nearly transform-limited Gaussian pulse of duration $\Delta T = 4$ fs (gray dashed curves), the small deviations being caused by small fourth-order dispersion in the lens. In addition, Figs. 5(b) and (c) evidence that not only the envelope but also the electric field does not change appreciably in the first half of the focus because the CEP is approximately constant in this region.

5 Conclusions

To summarize, we have shown that lenses can be used to focus to transform-limited, few-cycle pulses with propagation-invariant envelope shape along the focus, and with partially frozen carrier-envelope phase. First, if the illuminated lens area is small enough for aperture and spherical aberration effects to be negligible, elimination of the dispersive effects of the lens amounts to eliminate the dispersive effects of a slab of thickness equal to the lens central thickness, which is technically possible by dispersion pre-compensation for input pulses with several cycles for typical lens thicknesses, and for pulses close to the limit of a single cycle for particularly thin lenses. Second, the nearly transform-limited pulse after the lens obtained by pre-

compensation remains transform-limited and propagates undistorted along the focal region if the lens chromatic aberration is small. Given a lens material, a focal depth and the pulse duration, this condition is characterized by Eq. (10). Within these conditions, we have found the simple expression in Eq. (19) for the carrier-envelope phase shift experienced by the pulse along the focal region. Finally, the specific small chromatic aberration introduced by focusing with the focal length and input spot size given by Eq. (22) results in a constant carrier-envelope phase in any desired half focal depth, and therefore in an electric field with constant temporal shape in that half focal depth. All these situations can be given at usual carrier wavelengths using common lens glasses or crystals, and with input spot sizes and focal lengths of the same order as those typically used in experiments involving focusing of few-cycle pulses for phase-sensitive interactions with matter. The validity of these conclusions has been verified from a realistic wave model of lens focusing in which the lens variable thickness and material dispersion, lens aperture, spherical and chromatic aberrations are accurately taken into account.

References

1. C. A. Haworth, L. E. Chipperfield, J. S. Robinson, P. L. Knight, J. P. Marangos and J. W. G. Tisch, "Half-cycle cutoffs in harmonic spectra and robust carrier-envelope phase retrieval," Nature Physics **3,** 52-57 (2007).
2. M. Schnñurer, Z. Cheng, M. Hentschel, F.Krausz, T.Wilhein, D.Hambach, G. Schmahl, M. Drescher, Y. Lim, U. Heinzmann, "Few-cycle-driven XUV laser harmonics: generation and focusing," Appl. Phys. B **70,** S227S232 (2000).
3. F. Krausz and Misha Yu. Ivanov, "Attosecond Physics," Rev. Mod. Phys. **81,** 161-234 (2009).
4. M. Hentschel, R. Kienberger, Ch. Spielmann, G. A. Reider, N. Milosevic, T. Brabec, P. Corkum, U. Heinzmann, M. Drescher, and F. Krausz, "Attosecond metrology," Nature **414,** 509-513 (2001).
5. A. Apolonski, P. Dombi, G.G. Paulus, M. Kakehata, R. Holzwarth, Th. Udem, Ch. Lemell, K. Torizuka, J. Burgdörfer, T. W. Hänsch,4 and F. Krausz, "Observation of Light-Phase-Sensitive Photoemission from a Metal," Phys. Rev. Lett. **92,** 073902 (2004).
6. S. E. Irvine, P. Dombi, G. Farkas, and A. Y. Elezzabi, "Influence of the carrier-envelope phase of few-cycle pulses on ponderomotive surface-plasmon acceleration," Phys. Rev. Lett. **97,** 146801 (2006).
7. T. Tritschler, K. D. Hof, M. W. Klein, and M. Wegener, "Variation of the carrier-envelope phase of few-cycle laser pulses owing to the Gouy phase: a solid-state-based measurement," Opt. Lett. **30,** 753-755 (2005).
8. T. M. Fortier, P. A. Ross, D. J. Jones, S. T. Cundiff, R. D. R. Bhat, and J. E. Sipe, "Carrier-envelope phase-controlled quantum interference of injected photocurrents in semiconductors," Phys. Rev. Lett. **92,** 147403 (2004).
9. T. Wittmann, B. Horvath, W. Helml, M. G. Schtzel, X. Gu, A. L. Cavalieri, G. G. Paulus, and R. Kienberger, "Single-shot carrierenvelope phase measurement of few-cycle laser pulses," Nature Physics **5,** 357 - 362 (2009).

10. G.G. Paulus, F. Lindner, H.Walther, A. Baltuska, E. Goulielmakis, M. Lezius, and F. Krausz, "Measurement of the Phase of Few-Cycle Laser Pulses," Phys. Rev. Lett. **91,** 253004 (2003).
11. F. Lindner, G.G. Paulus, H.Walther, A. Baltuska, E. Goulielmakis, M. Lezius, and F. Krausz, "Gouy Phase Shift for Few-Cycle Laser Pulses," Phys. rev. Lett. **92,** 113001 (2004).
12. S. A. Trushin, K. Kosma, W. Fuss, and W. E. Schmid, "Sub-10-fs supercontinuum radiation generated by filamentation of few-cycle 800 nm pulses in argon," Opt. Lett. **32,** 2432-2434 (2007).
13. C. P. Hauri, W. Kornelis, F. W. Helbing, A. Heinrich, A. Couairon, A. Mysyrowicz, J. Biegert, U. Keller, "Generation of intense, carrier-envelope phase-locked few-cycle laser pulses through filamentation," Appl. Phys. B **79,** 673677 (2004).
14. P. Salieres, A. L'Huillier, and M. Lewenstein, "Coherence control of high-order harmonics," Phys. Rev. Lett. **74,** 3776- 3779 (1995).
15. M. A. Porras, "Characterization of the electric field of focused pulsed Gaussian beams for phase-sensitive interactions with matter," Opt. Lett. **34,** 1546-1548 (2009).
16. M. A. Porras, P. Dombi, "Freezing the carrier-envelope phase of few-cycle pulses about a focus," Opt. Express **17,** 19424-19434 (2009).
17. Zs. Bor, "Distortion of femtosecond laser pulses in lenses and lens systems," J. Mod. Opt. **35,** 1907-1918 (1988).
18. Zs. Bor and Z. L. Horváth, "Distortion of femtosecond pulses in lenses. Wave optical description," Opt. Commun. **94,** 249-258 (1992).
19. Z. L. Horváth and Zs. Bor, "Behavior of femtosecond pulses on the optical axis of a lens. Analytical description," Opt. Commun. **108,** 333-342 (1994).
20. M. Kempe and W. Rudolph, "Femtosecond pulses in the focal region of lenses," Phys. Rev. A **48,** 4721-4729 (1993).
21. M. Kempe, U. Stamm, B. Wilhelmi, and W. Rudolph, "Spatial and temporal transformation of femtosecond laser pulses by lenses and lens systems," J. Opt. Soc. Am B **9,** 1158-1965 (1992).
22. M. Kempe and W. Rudolph, "Impact of chromatic and spherical aberration on the focusing of ultrashort light pulses by lenses," Opt. Lett. **18,** 137-139 (1993).
23. J. J. Stamnes, *Waves in Focal Regions: Propagation, Diffraction and Focusing of Light, Sound and Water Waves,* Bristol, Hilger (1986).
24. M. Born and E. Wolf, *Principles of Optics,* Pergamon Press, Oxford (1987).
25. E. Hecht, *Optics,* Addison-Wesley (2002).
26. I. S. Gradshteyn and I. M. Ryzhik, *Table of integrals, series and products,* Academic, San Diego (1994).
27. See, for example, *Handbook of Optics,* Optical Society of America and Michael Bass, Eds., Vol. II (1994), or http://refractiveindex.info
28. See, for example, A. E. Siegman, *Lasers,* University Science books, Mill Valley, California (1986).
29. Edmund Optics and Optical Instruments Catalog 2011.
30. M. A. Porras, "Diffraction effects in few-cycle optical pulses," Phys. Rev. E **65,** 026606 (2002).
31. S. Feng and H. G. Winful, "Spatiotemporal structure of isodiffracting ultrashort electromagnetic pulses," Phys. Rev. E **61,** 862-873 (2000).
32. M. A. Porras, "Ultrashort pulsed Gaussian light beams," Phys. Rev. E **58,** 1086-1093 (1998).